# ASSESSMENT OF A NEXT GENERATION GRAVITY MISSION FOR MONITORING THE VARIATIONS OF EARTH'S GRAVITY FIELD

## TN5: MULTI-SATELLITE SIMULATION TOOL FOR SST MISSION

| ***Written by*** | ***Responsibility***<br>+ handwritten signature if no electronic workflow tool |
|---|---|
| F. Cossu | Author |
| | |
| | |
| ***Verified by*** | |
| A. Anselmi | Checker |
| | |
| ***Approved by*** | |
| A. Anselmi | Study Manager |
| | |
| ***Documentation Manager*** | |
| R. Cavaglià | |

Approval evidence is kept within the documentation management system.

## *CHANGE RECORDS*

| ISSUE | DATE | § CHANGE RECORDS | AUTHOR |
|---|---|---|---|
| draft | August 10 | | fc |

## TABLE OF CONTENTS

# 1. INTRODUCTION

## 1.1 Scope and Purpose

This document is submitted in fulfilment of WP 2310 of the Next Generation Gravity Mission (NGGM) study. Together with WP 2320 and WP 2330 it constitutes the output of Task 4 of the NGGM statement of work.

The objective of the WP 2310 is to realize an end-to-end numerical performance simulator with independent multi-satellite dynamics, compatible with all the relevant perturbation sources (e.g. static and variable gravity field).

This simulator is an evolution of the Mission Simulation Tool developed by TAS-I in the “System Support to Laser Interferometry Tracking Technology Development for Gravity Field Monitoring” [RD-5]. In particular, the evolution consists in the introduction in the simulator of a time-variable model of the Earth gravity field and in the generation of a series of outputs necessary to feed the “Backward Module” for the reconstruction of the geopotential from the observables produced by the space segment. Consequently, the original architecture and the operation procedures of the Mission Simulation Tool have been updated too. The new architecture and user procedures are described in [RD-24], while the present document provides:

- a brief description of the simulation scenarios;
- a description of the updates made to the simulator and of the new models added;
- a description of the performed simulations.

# 2. DOCUMENTS

## 2.1 Applicable Documents

[AD-1] Assessment of a Next Generation Gravity Mission to monitor the variations of Earth's gravity field, Statement of Work, EOP-SF/2008-09-1334, Issue 2, 20 November 2008, Appendix 1 to AO/1-5914/09/NL/CT

[AD-2] Special Conditions of Tender, Appendix 3 to AO/1-5914/09/NL/CT

[AD-3] Draft Contract. Appendix 2 to AO/1-5914/09/NL/CT.

## 2.2 ESA Reference Documents

[RD-1] Rummel et al. (2003), Scientific objectives for Future Geopotential Missions, Technical Note, Version 6 from the ESA contract No: 16668/02/NL/MM "Enabling Observation Techniques for Future Solid Earth Missions"

[RD-2] Koop, R., Rummel, R. (2007), The Future of Satellite Gravimetry, Final Report of the Future Gravity Mission Workshop, 12-13 April 2007 ESA/ESTEC, Noordwiik, Netherlands

[RD-3] Laser Doppler Interferometry Mission for determination of the Earth's Gravity Field, ESTEC Contract 18456/04/NL/CP, Final Report, Issue 1, 19 December 2005

[RD-4] Laser Interferometry High Precision Tracking for LEO, ESA Contract No. 0512/06/NL/IA, Final Report, July 2008

[RD-5] System Support to Laser Interferometry Tracking Technology Development for Gravity Field Monitoring, ESA Contract No. 20846/07/NL/FF, Final report, September 2008

[RD-6] Bender P.L., Wiese D.N., and Nerem R.S., "A Possible Dual-GRACE Mission With 90 Degree And 63 Degree Inclination Orbits", Proceedings of the 3rd International Symposium on Formation Flying, Missions and Technologies, Noordwijk (NL), April 2008

[RD-7] T. van Dam et al., Monitoring and Modelling Individual Sources of Mass Distribution and Transport in the Earth System by Means of Satellites, Final Report, ESA Contract No. 20403, November 2008

[RD-8] Variable Earth Model Description and Product Specification Document, ESA Contract No. 20403, November 2008

[RD-9] Enabling Observation Techniques for Future Solid Earth Missions, ESA Contract No: 16668/02/ NL/MM, Final report, Issue 2, 15 July 2004.A

## 2.3 NGGM Study Notes

[RD-10] NGGM TN1 "Requirement Analysis", University of Luxembourg, Issue 1, Revision 1, 8 February 2010

[RD-11] NGGM TN2 "System Drivers", Thales Alenia Space, SD-TN-AI-1262, 4 December 2010

[RD-12] NGGM TN3 Part 1 "Observing Techniques and Instrument Concepts", Thales Alenia Space Italy, SD-TN-AI-1289, draft, July 2010

[RD-13] NGGM TN3 Part 2 "Observing Techniques", IAPG, 30 July 2010

[RD-14] NGGM TN3 Part 3 “Instrument Concepts”, ONERA, 1/16598 DMPH, draft, July 2010

[RD-15] NGGM TN4 Part 1 “Mission Analysis and AOCS concepts”, Thales Alenia Space Italy, SD-TN-AI-1290, draft, July 2010

[RD-16] NGGM TN4 Part 2 “NGGM Mission Analysis Report”, Deimos, NGGM-DME-TEC-TNO-01, July 2010

[RD-17] NGGM TN5 Part 1 “Multi-Satellite Simulation Tool for SST Mission”, Thales Alenia Space Italy, SD-TN-AI-1291, August 2010

[RD-18] NGGM TN5 Part 2 “Scientific Simulation Tool”, DEOS, WP2330-DEOS-v1, Issue 1, 12 August 2010

[RD-19] NGGM TN5 Part 3 “Reprocessing of Mass Transport Data”, IAPG, 17 August 2010

[RD-20] NGGM TN6 Part 1 “Mission Architecture Outlines”, Thales Alenia Space Italy, SD-TN-AI-1292, 30 July 2010

[RD-21] NGGM TN6 Part 2 “Scientific Assessment of Mission Architectures”, GIS, TN6-WP2420-GIS, July 2010

[RD-22] NGGM TN7 “Conclusions and Recommendations”, Thales Alenia Space Italy, to be initiated

## 2.4 Further Reference Documents

[RD-23] System Support To Laser Interferometry Tracking Technology Development For Gravity Field Monitoring, TR1: “Performance Analysis And Budget”, Thales Alenia Space Italy, SD-TN-AI-1108, 3 October 2008

[RD-24] System Support To Laser Interferometry Tracking Technology Development For Gravity Field Monitoring, TR3: “Simulator Design Document”, Thales Alenia Space Italy, SD-TN-AI-1158

[RD-25] ECSS, Space Engineering – Space Environment, ECSS-E-ST-10-04C, 15 November 2008

## 2.5 Reference websites

[RW-1] http://modelweb.gsfc.nasa.gov/atmos/nrlmsise00.html
[RW-2] http://sol.spacenvironment.net/~JB2006/

## 3. UPDATES TO THE SIMULATOR

**The simulator consists of a variety of models, each one having its own input files describing the features and the behaviour of the model. The block diagram of the models is shown in**

Figure 3-1.
During this study some model has been updated and a new one has been added. In particular the models updated are:

- ENVIRONMENT
- OUTSIDEWORLD
- ACC_TASI
- OPTM_TASI
- CTRL_TASI

while the new model added is:

- NGDAME_TASI

The names of the subsequent sections are followed, if applicable, by the name of the model that has been updated in parenthesis.

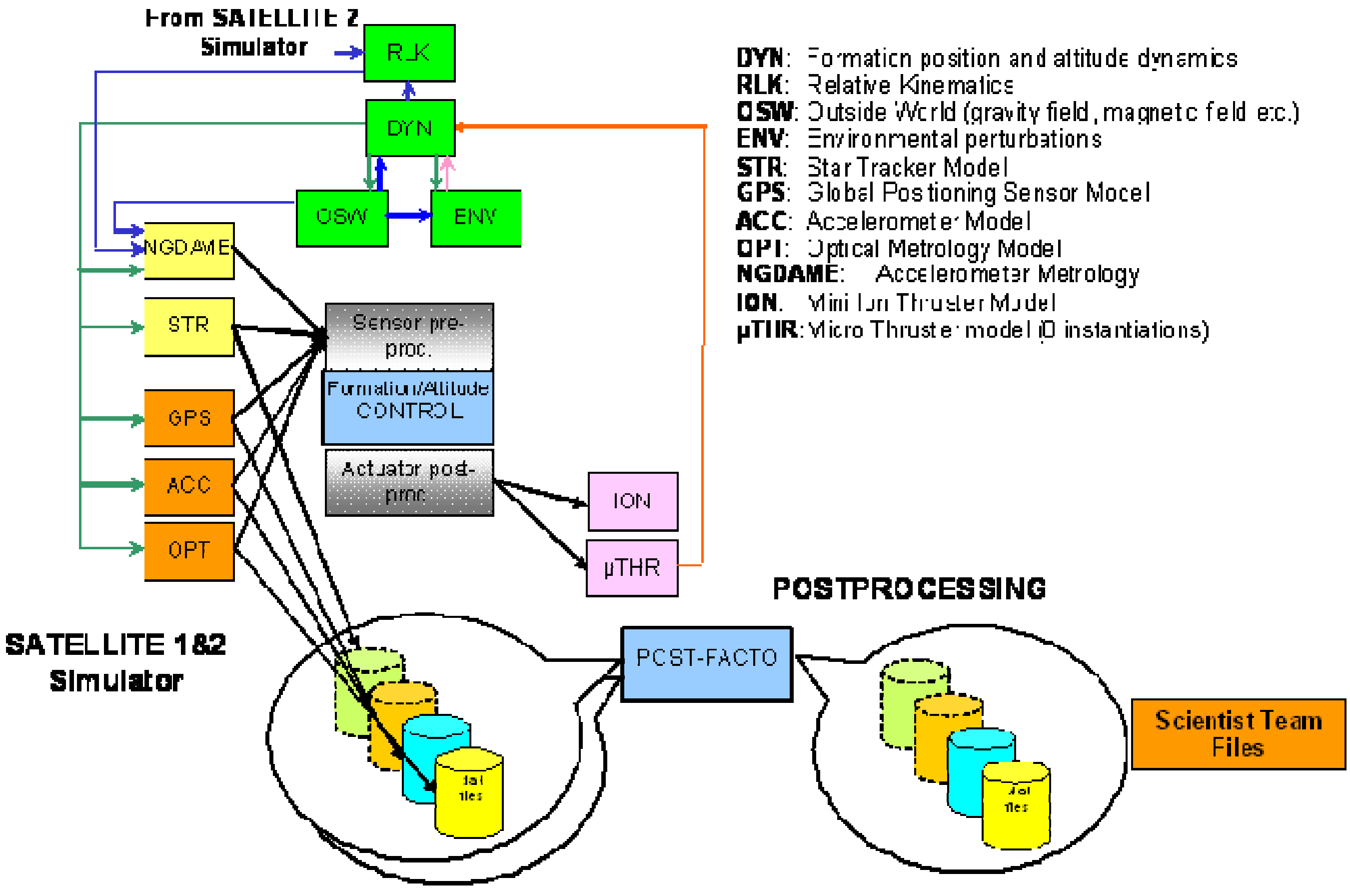


**Figure 3-1: Block diagram of the modules of the simulator.**

## 3.1 Environment model update (ENVIRONMENT)

The first model to be updated was the environment model which describes the external forces and torques acting on the satellites, depending on the geometry of the satellites. A new satellite geometry has been introduced. The central body consists of a prism of length L=3.25 m with the following trapezoidal base:

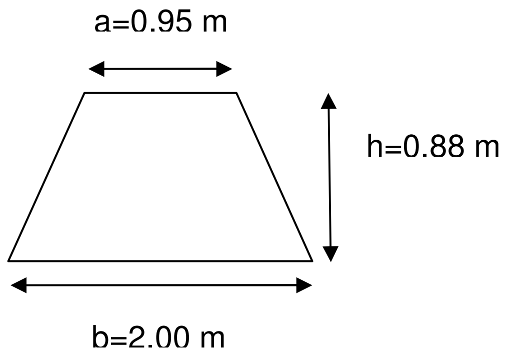


There are two solar panels attached to the central body of the same width as the side panels of the spacecraft, since they are initially folded. The total number of surfaces is 8: 2 trapezoids for the front and the back and 6 rectangles for the other surfaces. For each surface it was computed the area, the coordinates of the centre of pressure and the normal. The last geometric model of the satellites is shown in Figure 3-2.

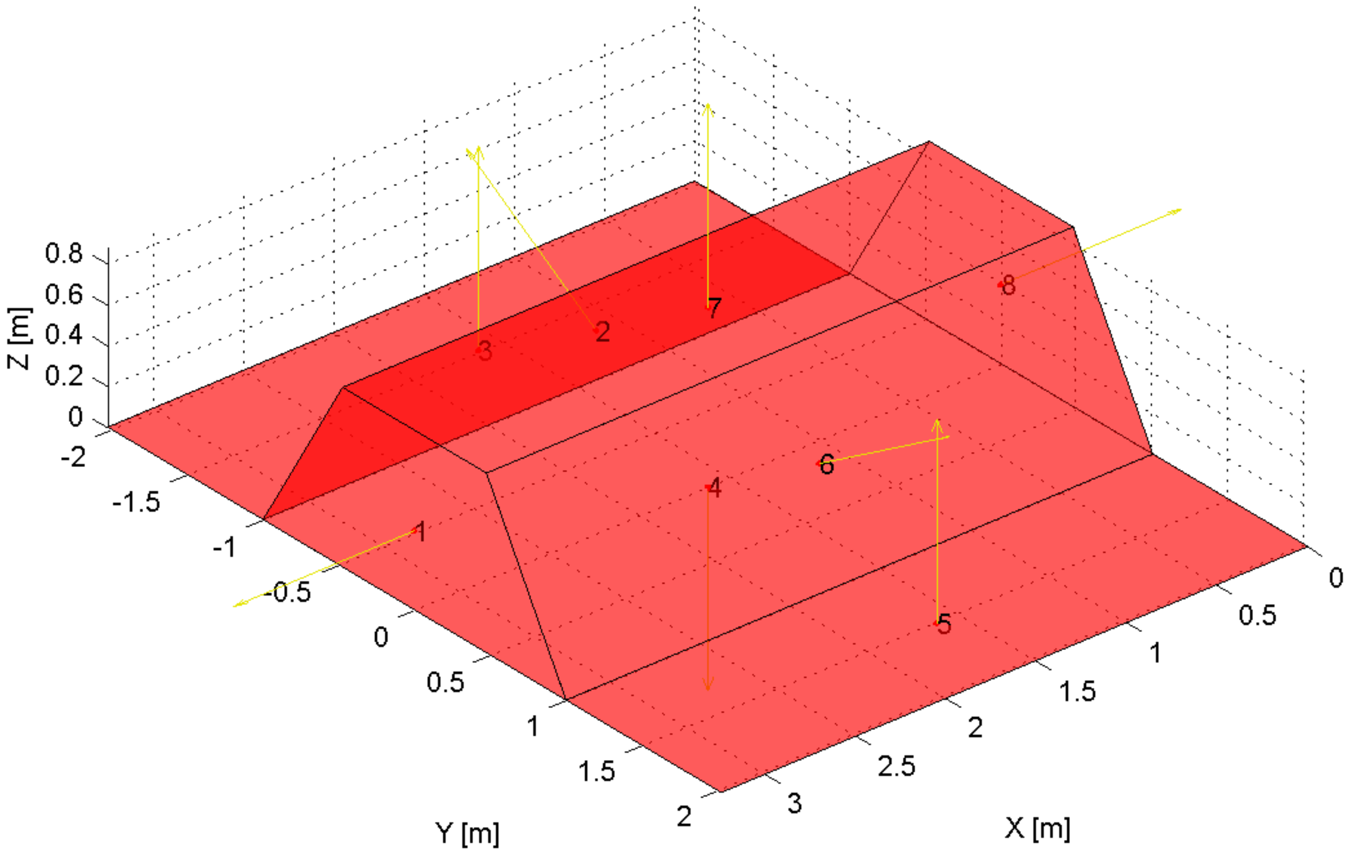


**Figure 3-2: New satellite geometry.**

## 3.2 Time-variable gravity field model (OUTSIDEWORLD)

The gravitational field is modelled with a series of spherical harmonics whose coefficients come from the EGM96 model. This static model was improved with a time-variable gravity model in which the coefficients of the spherical harmonics change with time. IAPG provided 28 data files containing spherical harmonic coefficients to degree and order 180 updated every 6 hours for one week starting at 01 Jan 1995 $00^{h}:00^{min}$. An option in the inputfile of this model allows the user to choose between static or time-variable gravity field.

## 3.3 Atmospheric density model update (OUTSIDEWORLD)

Following ECSS recommendations (see [RD-25], section 7.1.3), the NRLMSISE-00 model (NRL Mass Spectrometer, Incoherent Scatter Radar Extended Model 2000) must be used for calculating both the neutral temperature and the detailed composition of the atmosphere, while the JB-2006 model (Jacchia-Bowman model 2006) must be used for calculating the total atmospheric density above an altitude of 120 km.

Until now, the NRLMSISE-90 model has been used for calculating all the quantities specified above. We updated this model with the NRLMSISE-00 model (see [RW-1]) and with the JB-2006 model (see [RW-2]) and we made them work simultaneously to provide the necessary quantities.

## 3.4 Gravity gradient computation update (OUTSIDEWORLD)

The simulator was capable of computing analytically the gravity gradient tensor at any point of the orbit using a gravity field approximated to the J2 term. This tensor was used to compute the gravitational torque on the satellites and for this purpose its degree of approximation was sufficient. To make the control loop more realistic, it had to be fed with more realistic acceleration measurements coming from the accelerometers test masses taking also into account gravity gradient terms. For this purpose a higher degree of approximation in the computation of the gravity gradient tensor was needed. Starting from a grid of pre-computed values (with degree and order 360) in the range 194 km – 404 km with a resolution of 1/8 degrees in latitude and longitude and of 7 km in height , the values of the gravity gradient tensor are now computed by interpolating the pre-computed values in the desired spatial point.

## 3.5 Accelerometers configuration update (ACC_TASI)

In the previous version of the simulator there was a couple of accelerometers for each axis of the satellite. Now the configuration is with one couple arranged along the y axis and one couple arranged along the z axis. Each accelerometer has two ultra sensitive axes and one less sensitive axis, as shown in Figure 3-3. The distance of each accelerometer from the centre of mass is 25 cm.

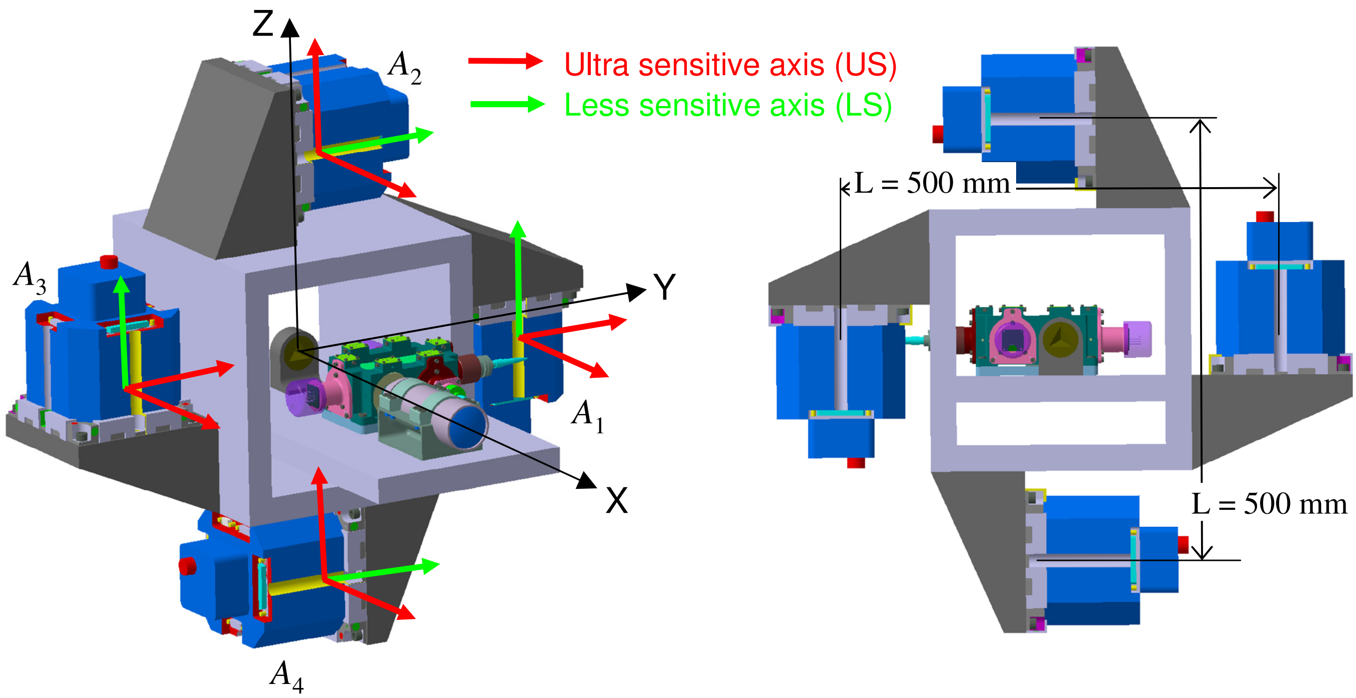


**Figure 3-3: Accelerometers configuration.**

### 3.6 Accelerometers measurement noise update (ACC_TASI)

The accelerometer measurement noise model for long-duration runs for ultra sensitive (US) and less sensitive (LS) axes was updated with the following profiles:

$$\tilde{n}_{US} \leq \begin{cases} 3\cdot 10^{-12} & \text{for } f \geq 0.001 \text{ and } f \leq 0.1\,\text{Hz} \\ 3\cdot 10^{-12}\cdot\left(\dfrac{0.001}{f}\right)^2 & \text{for } f < 0.001\,\text{Hz} \\ 3\cdot 10^{-12}\cdot\left(\dfrac{f}{0.01}\right)^2 & \text{for } f > 0.1\,\text{Hz} \\ 3\cdot 10^{-8} & \text{for } f < 10^{-5}\,\text{Hz} \end{cases} \quad \frac{\text{m}}{\text{s}^2\sqrt{\text{Hz}}}$$

$$\tilde{n}_{LS} \leq \begin{cases} 3\cdot 10^{-10} & \text{for } f \geq 0.001 \text{ and } f \leq 0.1\,\text{Hz} \\ 3\cdot 10^{-10}\cdot\left(\dfrac{0.001}{f}\right)^2 & \text{for } f < 0.001\,\text{Hz} \\ 3\cdot 10^{-10}\cdot\left(\dfrac{f}{0.01}\right)^2 & \text{for } f > 0.1\,\text{Hz} \\ 3\cdot 10^{-6} & \text{for } f < 10^{-5}\,\text{Hz} \end{cases} \quad \frac{\text{m}}{\text{s}^2\sqrt{\text{Hz}}}$$

The profiles obtained from the simulator are shown in Figure 3-4.

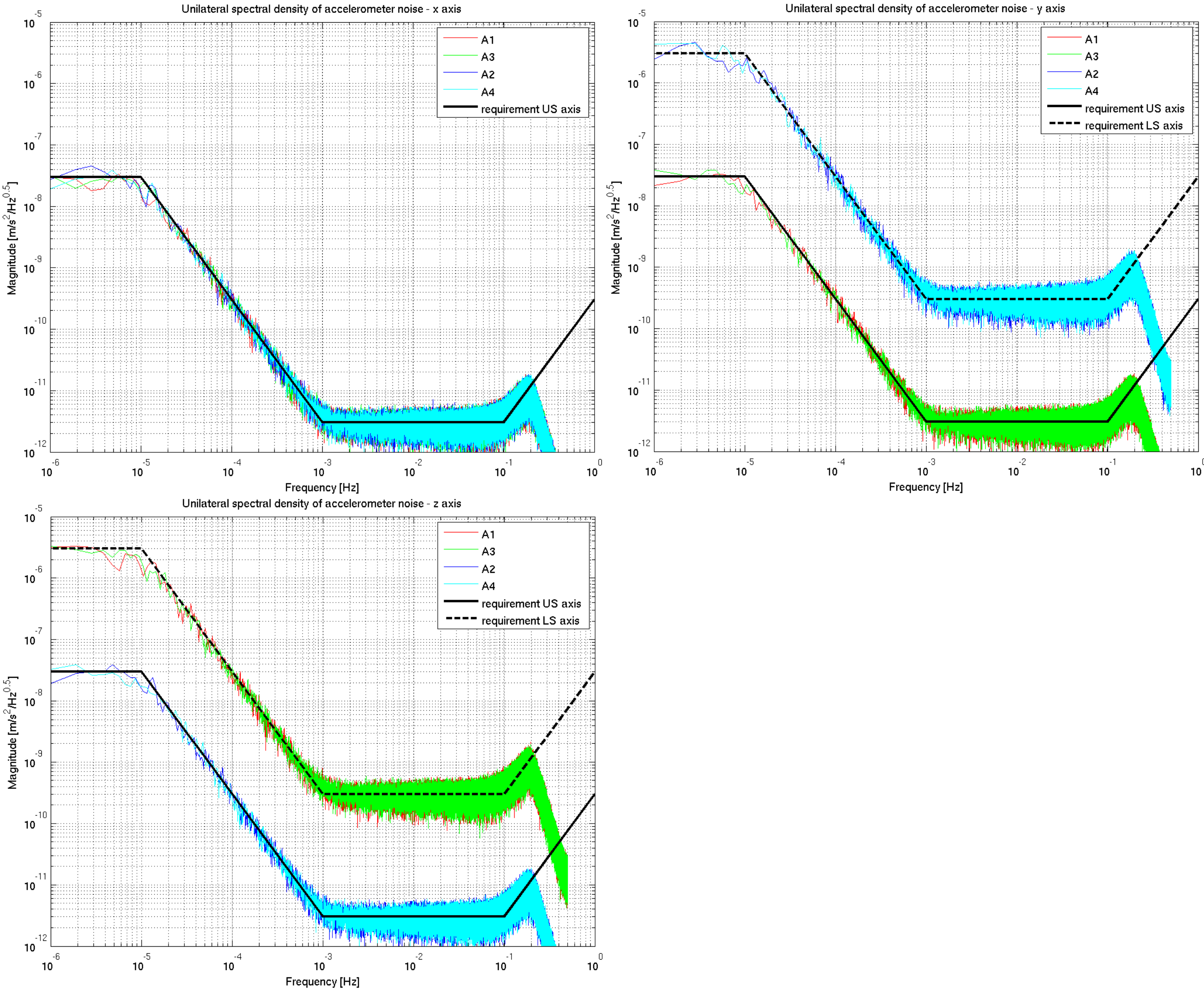


**Figure 3-4: accelerometers noise profiles for x, y and z axes.**

## 3.7 Non-gravitational acceleration measurement error (NGDAME_TASI)

The measurement error on the non-gravitational differential acceleration between the satellites, along the line joining the COM of the two satellites, was not included in the previous version of the simulator. The model for generating this error is described in section 5.2.

## 3.8 SS distance measurement error update (OPTM_TASI)

The measurement error on the satellite-to-satellite distance variation, along the line joining the COM of the two satellites, was updated with the model described in section 5.1.

## 3.9 Control laws update (CTRL_TASI)

New algorithms regarding drag-free control, formation control and attitude control have been implemented. For further details see chapter “CONTROL ARCHITECTURE AND DESIGN UPDATES” of [RD-15].

## 3.10 Angular rate and attitude reconstitution

A new offline emulator has been implemented to improve the fidelity of the estimated attitudes and angular rates of the satellites by making a "data fusion" between star tracker and accelerometers measurements. This emulator is also called "post-facto" emulator. For further details see chapter "POST-PROCESSING EMULATOR" of [RD-15].

## 3.11 Outputs for the Backward Module

A new set of output files have been prepared as input to the Backward Module (WP 2330, [RD-18]). The format of the data is Ascii and the file extension is "*.dat". The first part of the name of the files describes the type of formation (inline, pendulum or cartwheel), the type of orbit (polar, bender or SSO) and the duration of the simulation (in days), all separated by an underscore. The other part of the name of the files is one of the following names:

- file1
- file2a_1
- file2b_1
- file2a_2
- file2b_2
- file3_1_ECI
- file3_1_ECF
- file3_2_ECI
- file3_2_ECF
- file4_1
- file4_2

The terminating suffix "_1" or "_2" indicates a file with quantities coming from satellite 1 or satellite 2 respectively. The first column of all files contains the GPS time, while the variables present in the other columns are described in the header files of each file. The name of the header files starts with a "H" followed by the same name of the file they are referring to. For example the file named "inline_polar_37days_file1.dat" contains the variables specified in the header file "Hinline_polar_37days_file1.dat".

The time step between one record and the other is 1 s, while the time step of the series of data generated by the simulator is 0.1 s, so, to avoid aliasing, an anti-aliasing filter must be applied to those variables which contain frequencies higher than 0.5 Hz. A 7th order low-pass Butterworth filter with a cutoff frequency of 0.2 Hz was applied to those variables. The files that were processed with the anti-aliasing filter are indicated in the readme file provided with each simulation. An inverse filter called "inv_anti_aliasing_10Hz.txt" is provided so that the variables that have been filtered can be rephased.

As previously said, a readme file accompanies each simulation. It contains information about the simulation start time, the kind of scenario, the state vectors of the satellites, the duration of the simulation, the number of spherical harmonics used to compute the gravity field, the controls that were active, the name of the data files and their header files, information about the filtering and about the "post-facto" emulator variables, and the date of the delivery.

# 4. SIMULATIONS PERFORMED

For this study 5 different scenarios provided by DEOS have been investigated:

- scenario 1: inline formation, polar orbit;
- scenario 2: inline formation, inclined orbit (Bender type);
- scenario 3: inline formation, sun synchronous orbit;
- scenario 4: pendulum formation, polar orbit;
- scenario 5: cartwheel formation, polar orbit.

For each scenario DEOS provided the epoch and the state vector of the satellites both in rectangular inertial coordinates and as Keplerian elements. A total of 5 simulations have been performed, one for each scenario.

## 4.1 Simulations duration

The duration of the simulations needed to be equal to the orbit repeat period plus 5 days, so it was set to 36 days for scenario 2 and to 37 days for all the others. The actual printing to file starts after one day, to exclude the transient effects of the control algorithms, therefore the simulation covers a total time span of 37 (scenario 2) and 38 days (other scenarios).

## 4.2 Initial conditions

The initial conditions (state vectors) provided by DEOS are shown in Table 1. For each scenario the first six rows contain the inertial rectangular positions and velocities for satellite 1 and 2, while the other six rows contain the Keplerian elements (semi-major axis, eccentricity, inclination, right ascension of the ascending node, argument of perigee, mean anomaly). The epoch is the same for all scenarios.

| Start Time: 1 January 1996 00:00:00 UTC | | |
|---|---|---|
| | Sat 1 | Sat 2 |
| Scenario 1: | | |
| x [m] | 0.67123316708847e+07 | 0.67119854617125e+07 |
| y [m] | 0.57053473876977e+03 | 0.57498465863913e+03 |
| z [m] | -0.13410989479890e+05 | 0.61686672602566e+05 |
| $v_x$ [m/s] | 0.75983728191390e+01 | -0.78676917908920e+02 |
| $v_y$ [m/s] | 0.49712669155262e+00 | 0.48959354719164e+00 |
| $v_z$ [m/s] | 0.77119998484428e+04 | 0.77116887961020e+04 |
| a [m] | 6722739.1928 | 6722737.7670 |
| e [-] | 0.001848241012 | 0.001856992648 |
| i [deg] | 89.996311437 | 89.996312722 |
| Ω [deg] | 0.004877396 | 0.004874375 |
| ω [deg] | 33.167997895 | 33.594731398 |
| M [deg] | 326.833617786 | 327.047805778 |
| Scenario 2: | | |
| x [m] | 0.67356597657287e+07 | 0.67352454470903e+07 |

| | | |
|---|---|---|
| y [m] | -0.27038755896053e+04 | 0.31370692178143e+05 |
| z [m] | 0.81393325610148e+03 | 0.67640886961241e+05 |
| $v_x$ [m/s] | 0.43065374463912e+00 | -0.85349674466149e+02 |
| $v_y$ [m/s] | 0.34909416610088e+04 | 0.34907594141109e+04 |
| $v_z$ [m/s] | 0.68564658577818e+04 | 0.68560292439395e+04 |
| a [m] | 6737956.2510 | 6737954.6608 |
| e [-] | 0.000341240993 | 0.000342220572 |
| i [deg] | 63.017267061 | 63.017260540 |
| Ω [deg] | 359.973474812 | 359.973897545 |
| ω [deg] | 3.112947060 | 5.809065054 |
| M [deg] | 356.896939922 | 354.840137687 |
| Scenario 3: | | |
| x [m] | 0.66229859865818e+07 | 0.66241903042749e+07 |
| y [m] | 0.11700966865700e+07 | 0.11612081752972e+07 |
| z [m] | -0.10656068376968e+05 | 0.63896412726384e+05 |
| $v_x$ [m/s] | 0.16566454678989e+03 | 0.80949467365173e+02 |
| $v_y$ [m/s] | -0.90315647012142e+03 | -0.91806347802553e+03 |
| $v_z$ [m/s] | 0.76490667877446e+04 | 0.76487256761965e+04 |
| a [m] | 6735206.7965 | 6735205.8971 |
| e [-] | 0.001636983943 | 0.001644740642 |
| i [deg] | 96.845104817 | 96.845094438 |
| Ω [deg] | 10.008277796 | 10.008165446 |
| ω [deg] | 28.934541202 | 29.437449035 |
| M [deg] | 331.064946643 | 331.201769141 |
| Scenario 4: | | |
| x [m] | 0.67123316708826e+07 | 0.67118166310529e+07 |
| y [m] | 0.57053473979019e+03 | 0.62499523051353e+05 |
| z [m] | -0.13410989553073e+05 | 0.48689926819096e+05 |
| $v_x$ [m/s] | 0.75983729031449e+01 | -0.63738161725003e+02 |
| $v_y$ [m/s] | 0.49712669172502e+00 | -0.11103966371540e+00 |
| $v_z$ [m/s] | 0.77119998484448e+04 | 0.77118094479997e+04 |
| a [m] | 6722739.1928 | 6722738.1419 |
| e [-] | 0.001848241015 | 0.001854595240 |
| i [deg] | 89.996311437 | 89.996415719 |
| Ω [deg] | 0.004877395 | 0.533489080 |
| ω [deg] | 33.167997786 | 33.495358918 |
| M [deg] | 326.833617914 | 327.036120022 |
| Scenario 5: | | |
| x [m] | 0.67022539842682e+07 | 0.67222683278592e+07 |
| y [m] | 0.56594532247310e+03 | 0.57639472969745e+03 |
| z [m] | -0.58608155262552e+05 | 0.31816403469237e+05 |
| $v_x$ [m/s] | 0.33639586492871e+02 | -0.18323805570640e+02 |
| $v_y$ [m/s] | 0.50033587898675e+00 | 0.49438231960953e+00 |
| $v_z$ [m/s] | 0.77232364082366e+04 | 0.77005034067512e+04 |

| | | |
|---|---|---|
| a [m] | 6722766.7006 | 6722709.4379 |
| e [-] | 0.005323470482 | 0.002354030405 |
| i [deg] | 89.996309419 | 89.996309899 |
| Ω [deg] | 0.004870344 | 0.004895253 |
| ω [deg] | 55.278685747 | 271.460789244 |
| M [deg] | 304.723590357 | 88.540709001 |

**Table 1: Initial conditions for the 5 scenarios.**

The initial conditions determine the type of orbit and the formation followed by the two satellites, as one can see from Table 2.

| | formation | orbit | baseline (km) | repeat period (days) | sub-cycles (days) |
|---|---|---|---|---|---|
| Scenario 1 | inline | polar | 75 km | 32/503 | 4 & 7 |
| Scenario 2 | inline | Bender (63°) | 75 km | 31/481 | |
| Scenario 3 | inline | SSO | 75 km | 32/503 | 4 & 7 |
| Scenario 4 | pendulum | polar | 62/62 km | 32/503 | 4 & 7 |
| Scenario 5 | cartwheel | polar | 50/100 km | 32/503 | 4 & 7 |

**Table 2: Type of orbit and formation for the 5 scenarios.**

### 4.3 Offline processing

After a simulation is complete, two dedicated files containing the true quaternions, true angular velocities, true angular accelerations and the noises of the linear acceleration measurements made by the four accelerometers for the two satellites are first processed to "rephase" the variables with the inverse filter and then passed to the "post-facto" emulator, which generates the reconstituted attitudes (in ECI frame), angular velocities and angular accelerations for the two satellites (files "file3_1_ECI" and "file3_2_ECI"). A transformation of the true quaternions and of the reconstituted attitudes from ECI frame to ECF frame is also performed (files "file3_1_ECF" and "file3_2_ECF"). Since the application of the inverse filter generates some edge effects in the data series, the first and the last 30 points are excluded so that the epoch of the first record corresponds to 2 January 1996 00:00:30 UTC (GPS Time = 504576041 s).

### 4.4 Outputs generated

The outputs generated by the simulator to feed the Backward Module ([RD-18]) are divided into 11 different files, as anticipated in section 3.11. The variables contained in each file are listed in Table 3.

| Filename | Variable name | Units |
|---|---|---|
| file1: | | |
| | GPS_Time | [s] |
| | SS_DistanceMeasurementError | [m] |
| | NonGravDiffAccelMeasErr | [m/s^2] |
| file2a_1: | | |
| | GPS_Time | [s] |

| | | |
|---|---|---|
| | CaseSensorAcceleration_X_1 | [m/s^2] |
| | CaseSensorAcceleration_Y_1 | [m/s^2] |
| | CaseSensorAcceleration_Z_1 | [m/s^2] |
| | TestMass2_LinAcc_Ideal_X_1 | [m/s^2] |
| | TestMass2_LinAcc_Ideal_Y_1 | [m/s^2] |
| | TestMass2_LinAcc_Ideal_Z_1 | [m/s^2] |
| | TestMass3_LinAcc_Ideal_X_1 | [m/s^2] |
| | TestMass3_LinAcc_Ideal_Y_1 | [m/s^2] |
| | TestMass3_LinAcc_Ideal_Z_1 | [m/s^2] |
| | TestMass5_LinAcc_Ideal_X_1 | [m/s^2] |
| | TestMass5_LinAcc_Ideal_Y_1 | [m/s^2] |
| | TestMass5_LinAcc_Ideal_Z_1 | [m/s^2] |
| | TestMass6_LinAcc_Ideal_X_1 | [m/s^2] |
| | TestMass6_LinAcc_Ideal_Y_1 | [m/s^2] |
| | TestMass6_LinAcc_Ideal_Z_1 | [m/s^2] |
| file2b_1: | | |
| | GPS_Time | [s] |
| | TestMass2_LinAcc_Noise_X_1 | [m/s^2] |
| | TestMass2_LinAcc_Noise_Y_1 | [m/s^2] |
| | TestMass2_LinAcc_Noise_Z_1 | [m/s^2] |
| | TestMass3_LinAcc_Noise_X_1 | [m/s^2] |
| | TestMass3_LinAcc_Noise_Y_1 | [m/s^2] |
| | TestMass3_LinAcc_Noise_Z_1 | [m/s^2] |
| | TestMass5_LinAcc_Noise_X_1 | [m/s^2] |
| | TestMass5_LinAcc_Noise_Y_1 | [m/s^2] |
| | TestMass5_LinAcc_Noise_Z_1 | [m/s^2] |
| | TestMass6_LinAcc_Noise_X_1 | [m/s^2] |
| | TestMass6_LinAcc_Noise_Y_1 | [m/s^2] |
| | TestMass6_LinAcc_Noise_Z_1 | [m/s^2] |
| file2a_2: | | |
| | GPS_Time | [s] |
| | CaseSensorAcceleration_X_2 | [m/s^2] |
| | CaseSensorAcceleration_Y_2 | [m/s^2] |
| | CaseSensorAcceleration_Z_2 | [m/s^2] |
| | TestMass2_LinAcc_Ideal_X_2 | [m/s^2] |
| | TestMass2_LinAcc_Ideal_Y_2 | [m/s^2] |
| | TestMass2_LinAcc_Ideal_Z_2 | [m/s^2] |
| | TestMass3_LinAcc_Ideal_X_2 | [m/s^2] |
| | TestMass3_LinAcc_Ideal_Y_2 | [m/s^2] |
| | TestMass3_LinAcc_Ideal_Z_2 | [m/s^2] |
| | TestMass5_LinAcc_Ideal_X_2 | [m/s^2] |
| | TestMass5_LinAcc_Ideal_Y_2 | [m/s^2] |
| | TestMass5_LinAcc_Ideal_Z_2 | [m/s^2] |
| | TestMass6_LinAcc_Ideal_X_2 | [m/s^2] |
| | TestMass6_LinAcc_Ideal_Y_2 | [m/s^2] |
| | TestMass6_LinAcc_Ideal_Z_2 | [m/s^2] |
| file2b_2: | | |

| | | |
|---|---|---|
| | GPS_Time | [s] |
| | TestMass2_LinAcc_Noise_X_2 | [m/s^2] |
| | TestMass2_LinAcc_Noise_Y_2 | [m/s^2] |
| | TestMass2_LinAcc_Noise_Z_2 | [m/s^2] |
| | TestMass3_LinAcc_Noise_X_2 | [m/s^2] |
| | TestMass3_LinAcc_Noise_Y_2 | [m/s^2] |
| | TestMass3_LinAcc_Noise_Z_2 | [m/s^2] |
| | TestMass5_LinAcc_Noise_X_2 | [m/s^2] |
| | TestMass5_LinAcc_Noise_Y_2 | [m/s^2] |
| | TestMass5_LinAcc_Noise_Z_2 | [m/s^2] |
| | TestMass6_LinAcc_Noise_X_2 | [m/s^2] |
| | TestMass6_LinAcc_Noise_Y_2 | [m/s^2] |
| | TestMass6_LinAcc_Noise_Z_2 | [m/s^2] |
| file3_1_ECI: | | |
| | GPS_Time | [s] |
| | CoreQuaternion_1_1_ECI | [-] |
| | CoreQuaternion_2_1_ECI | [-] |
| | CoreQuaternion_3_1_ECI | [-] |
| | CoreQuaternion_4_1_ECI | [-] |
| | PostFactoAttitude_1_1_ECI | [-] |
| | PostFactoAttitude_2_1_ECI | [-] |
| | PostFactoAttitude_3_1_ECI | [-] |
| | PostFactoAttitude_4_1_ECI | [-] |
| | PostFactoCoreOmega_X_1 | [rad/s] |
| | PostFactoCoreOmega_Y_1 | [rad/s] |
| | PostFactoCoreOmega_Z_1 | [rad/s] |
| | PostFactoCoreOmegaDot_X_1 | [rad/s^2] |
| | PostFactoCoreOmegaDot_Y_1 | [rad/s^2] |
| | PostFactoCoreOmegaDot_Z_1 | [rad/s^2] |
| file3_1_ECF: | | |
| | GPS_Time | [s] |
| | CoreQuaternion_1_1_ECF | [-] |
| | CoreQuaternion_2_1_ECF | [-] |
| | CoreQuaternion_3_1_ECF | [-] |
| | CoreQuaternion_4_1_ECF | [-] |
| | PostFactoAttitude_1_1_ECF | [-] |
| | PostFactoAttitude_2_1_ECF | [-] |
| | PostFactoAttitude_3_1_ECF | [-] |
| | PostFactoAttitude_4_1_ECF | [-] |
| file3_2_ECI: | | |
| | GPS_Time | [s] |
| | CoreQuaternion_1_2_ECI | [-] |
| | CoreQuaternion_2_2_ECI | [-] |
| | CoreQuaternion_3_2_ECI | [-] |
| | CoreQuaternion_4_2_ECI | [-] |
| | PostFactoAttitude_1_2_ECI | [-] |
| | PostFactoAttitude_2_2_ECI | [-] |

| | | |
|---|---|---|
| | PostFactoAttitude_3_2_ECI | [-] |
| | PostFactoAttitude_4_2_ECI | [-] |
| | PostFactoCoreOmega_X_2 | [rad/s] |
| | PostFactoCoreOmega_Y_2 | [rad/s] |
| | PostFactoCoreOmega_Z_2 | [rad/s] |
| | PostFactoCoreOmegaDot_X_2 | [rad/s^2] |
| | PostFactoCoreOmegaDot_Y_2 | [rad/s^2] |
| | PostFactoCoreOmegaDot_Z_2 | [rad/s^2] |
| file3_2_ECF: | | |
| | GPS_Time | [s] |
| | CoreQuaternion_1_2_ECF | [-] |
| | CoreQuaternion_2_2_ECF | [-] |
| | CoreQuaternion_3_2_ECF | [-] |
| | CoreQuaternion_4_2_ECF | [-] |
| | PostFactoAttitude_1_2_ECF | [-] |
| | PostFactoAttitude_2_2_ECF | [-] |
| | PostFactoAttitude_3_2_ECF | [-] |
| | PostFactoAttitude_4_2_ECF | [-] |
| file4_1: | | |
| | GPS_Time | [s] |
| | OrbitPosition_X_1_ECF | [m] |
| | OrbitPosition_Y_1_ECF | [m] |
| | OrbitPosition_Z_1_ECF | [m] |
| | OrbitVelocity_X_1_ECF | [m/s] |
| | OrbitVelocity_Y_1_ECF | [m/s] |
| | OrbitVelocity_Z_1_ECF | [m/s] |
| file4_2: | | |
| | GPS_Time | [s] |
| | OrbitPosition_X_2_ECF | [m] |
| | OrbitPosition_Y_2_ECF | [m] |
| | OrbitPosition_Z_2_ECF | [m] |
| | OrbitVelocity_X_2_ECF | [m/s] |
| | OrbitVelocity_Y_2_ECF | [m/s] |
| | OrbitVelocity_Z_2_ECF | [m/s] |

**Table 3: Output files and variables generated by the simulator.**

The first column of each file is the GPS Time.

“file1” contains the satellite-to-satellite distance variation measurement error and the non-gravitational differential acceleration measurement error along the line joining the COMs of the two satellites.

“file2a_1” contains the true non-gravitational accelerations of the COM of satellite 1 along the three axes of the ACF (for a description of the reference frames definition, see ANNEX 1: REFERENCE FRAME DEFINITION of [RD-23]) and the ideal linear accelerations measured by the four accelerometers along the three axes of the ACF. These ideal accelerations consist of the true non-gravitational accelerations plus centrifugal accelerations. The effect of gravity gradients is not included. Also no noise is included. The accelerometers are named “TestMass2/3/5/6” following the convention of the previous configuration that included 6 accelerometers. Now, “TestMass2” corresponds to the accelerometer mounted along the positive y axis (A1 in Figure 3-3), “TestMass3” corresponds to the accelerometer mounted along the positive z axis (A2 in Figure 3-3), “TestMass5” corresponds to the accelerometer mounted along the negative y axis (A3 in Figure 3-3), “TestMass6” corresponds to the accelerometer mounted along the negative z axis (A4 in Figure 3-3).

“file2b_1” contains the linear acceleration measurement noises of the four accelerometers of satellite 1, whose spectral densities must correspond to those shown in Figure 3-4.

“file2a_2” and “file2b_2” contain the variables of satellite 2 analogous to those described above for satellite 1.

“file3_1_ECI” contains the true quaternions (in ECI frame) and the reconstituted attitudes (in ECI frame), angular velocities and angular accelerations generated by the “post-facto” module.

“file3_1_ECF” contains the true quaternions and reconstituted attitudes of “file3_1_ECI” converted in ECF frame.

“file3_2_ECI” and “file3_2_ECF” contains the same variables described above but for satellite 2.

“file4_1” contains the positions and velocities in ECF frame of satellite 1.

“file4_2” contains the positions and velocities in ECF frame of satellite 2.

Hereafter, a series of spectral density plots of some variables coming from the output files.

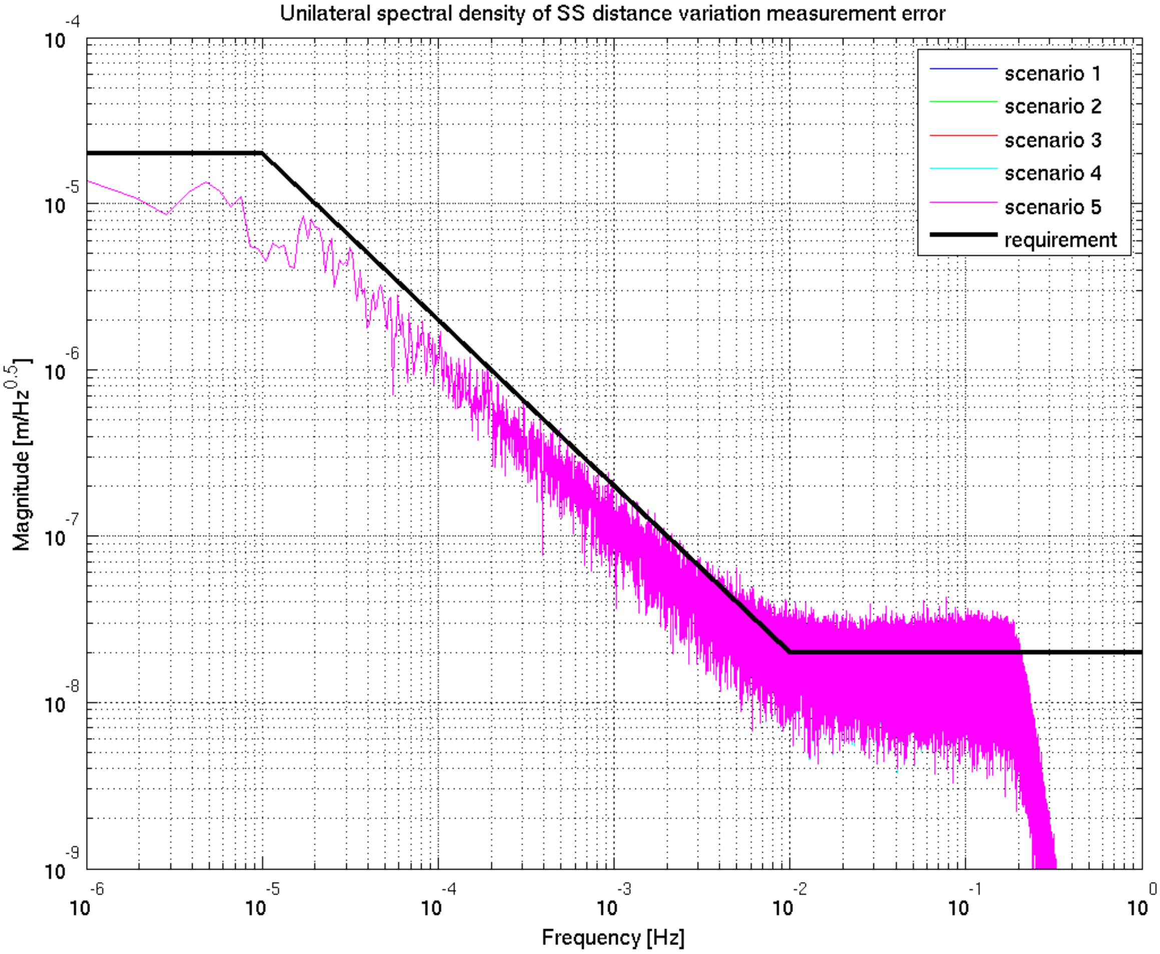


**Figure 4-1: satellite-to-satellite distance variation measurement error for the 5 scenarios.**

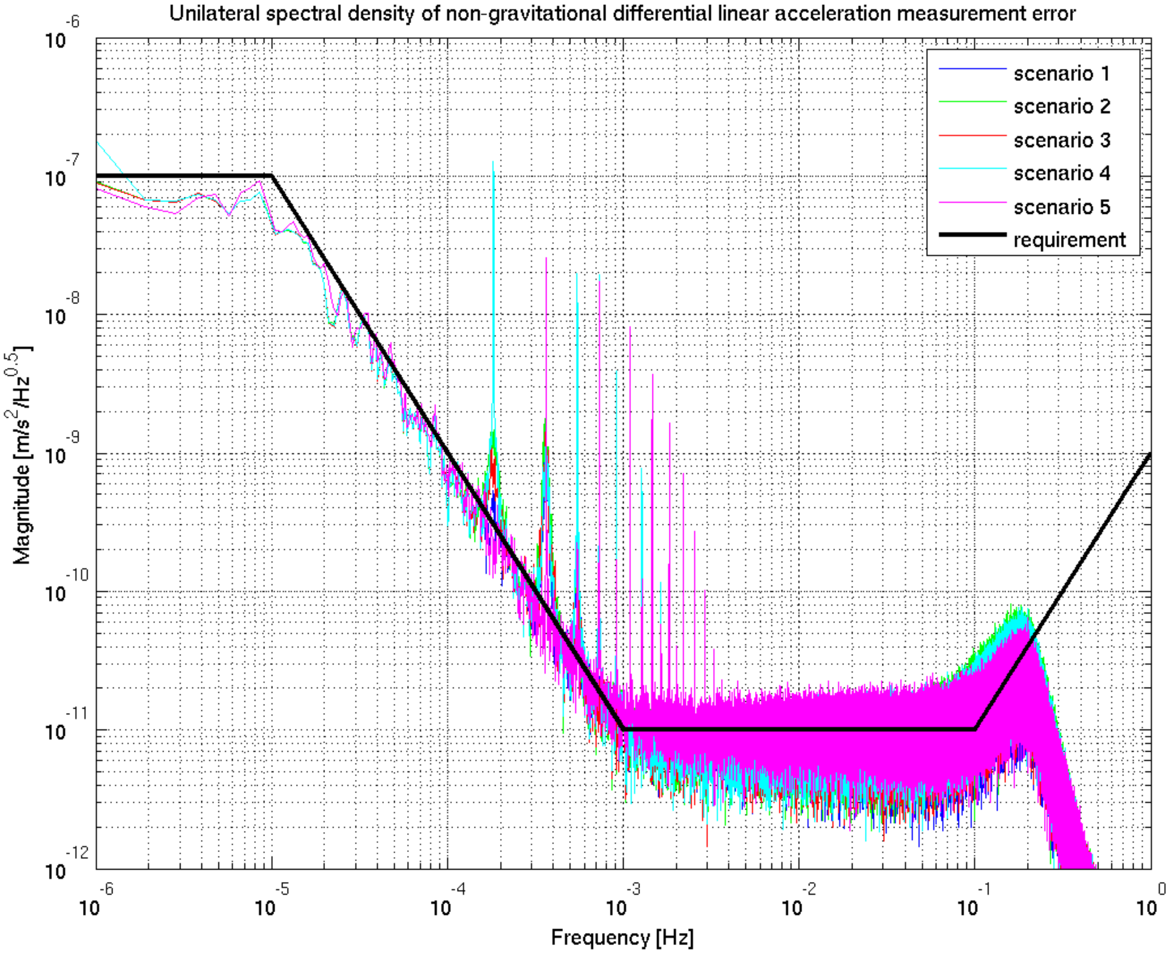


**Figure 4-2: unilateral spectral density of non-gravitational differential linear acceleration measurement error for the 5 scenarios.**

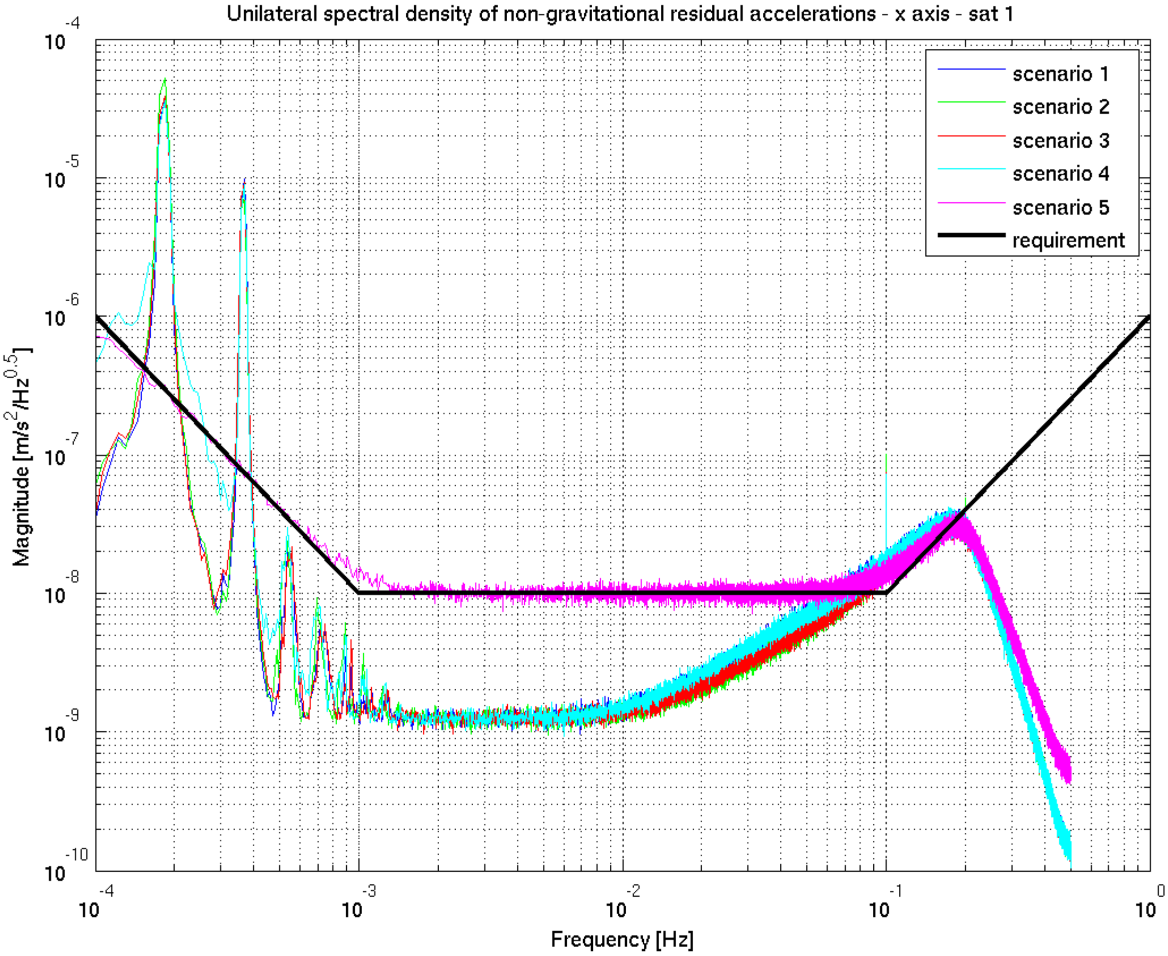


**Figure 4-3: unilateral spectral density of non-gravitational residual accelerations along x axis of satellite 1 for the 5 scenarios.**

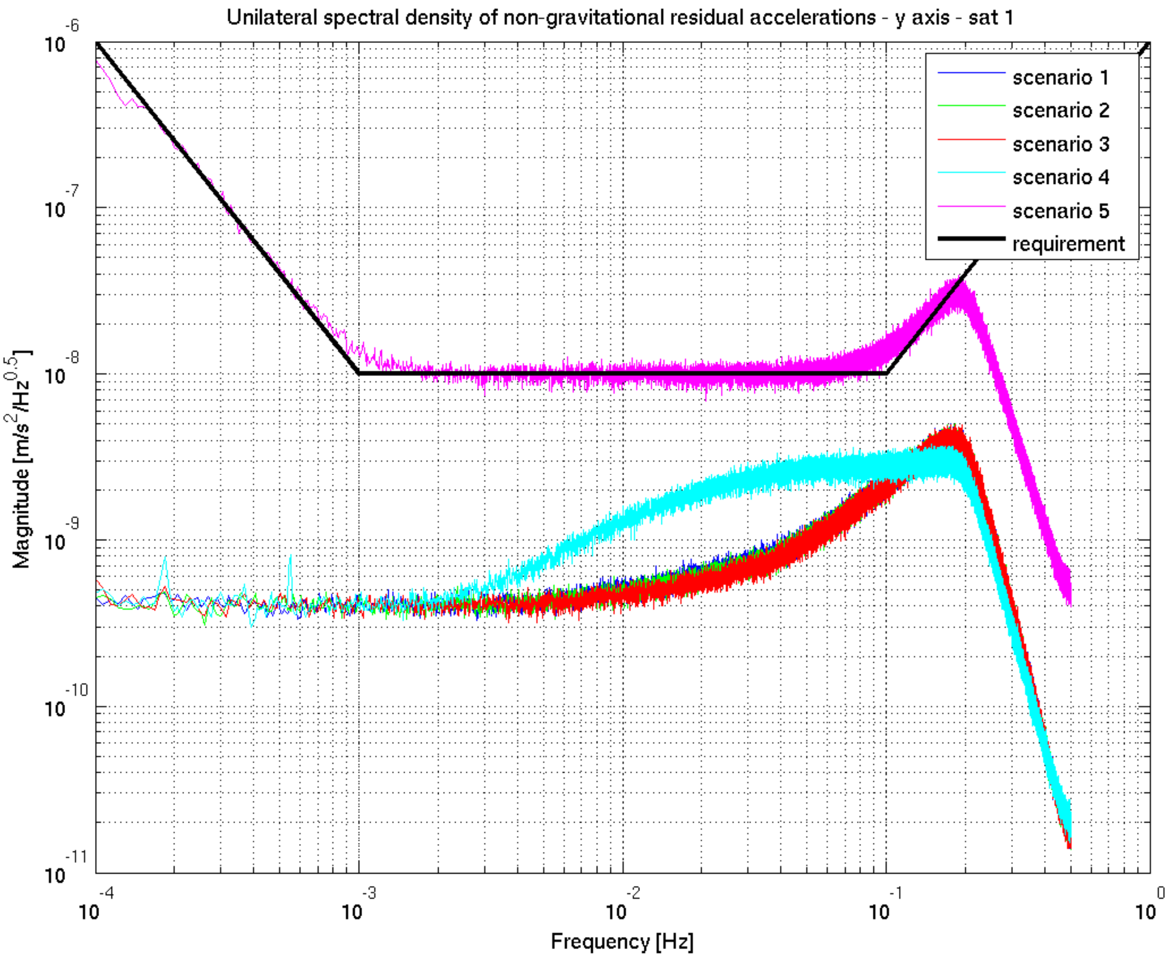


**Figure 4-4: unilateral spectral density of non-gravitational residual accelerations along y axis of satellite 1 for the 5 scenarios.**

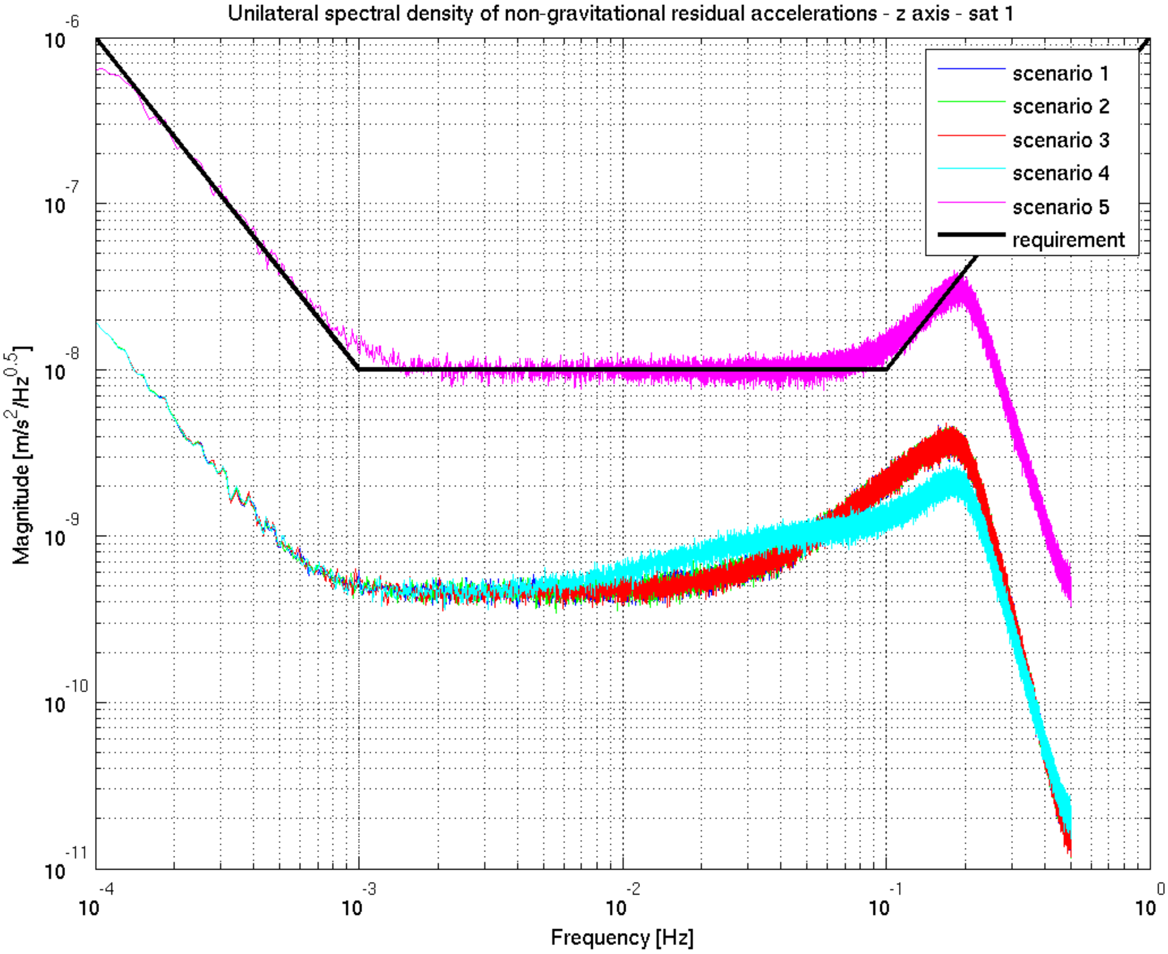


**Figure 4-5: unilateral spectral density of non-gravitational residual accelerations along z axis of satellite 1 for the 5 scenarios.**

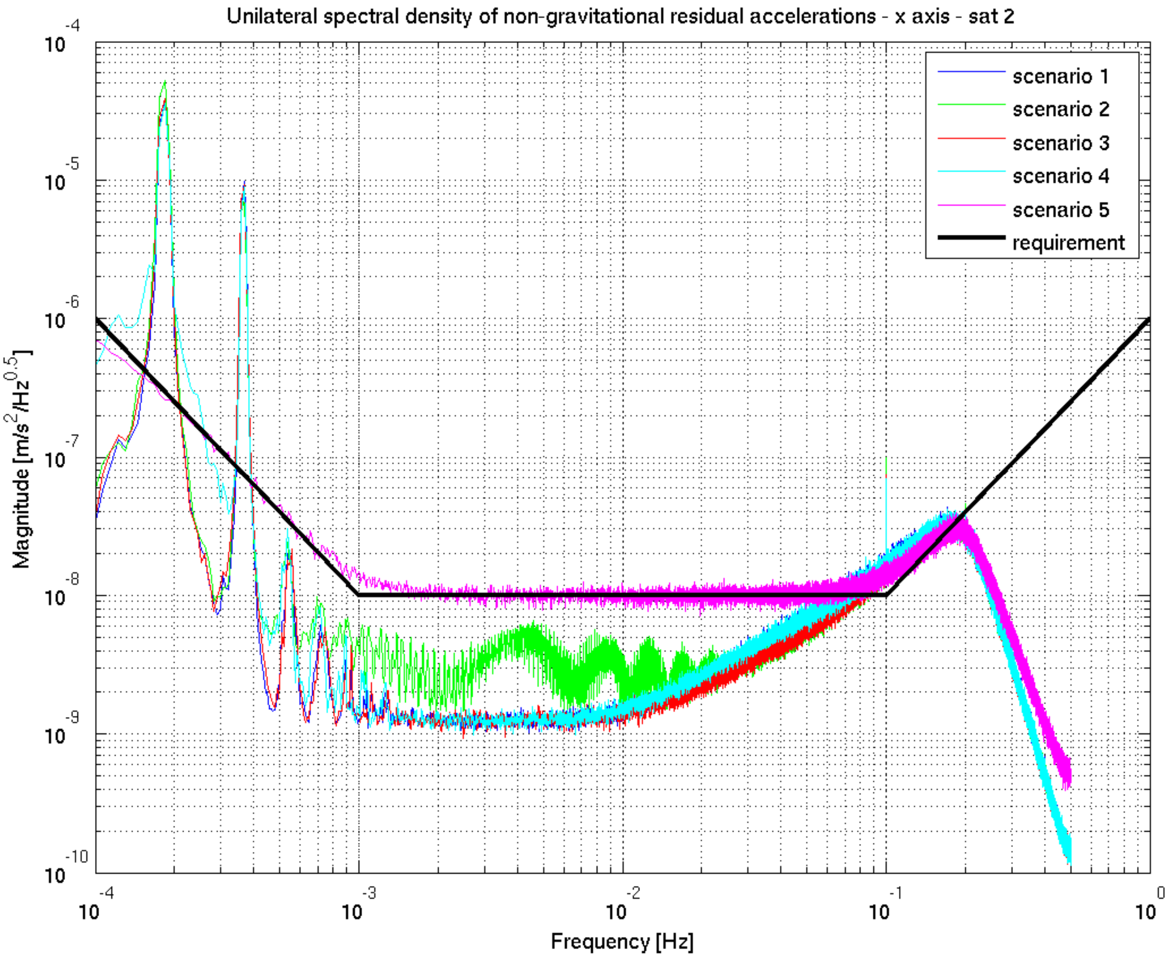


**Figure 4-6: unilateral spectral density of non-gravitational residual accelerations along x axis of satellite 2 for the 5 scenarios.**

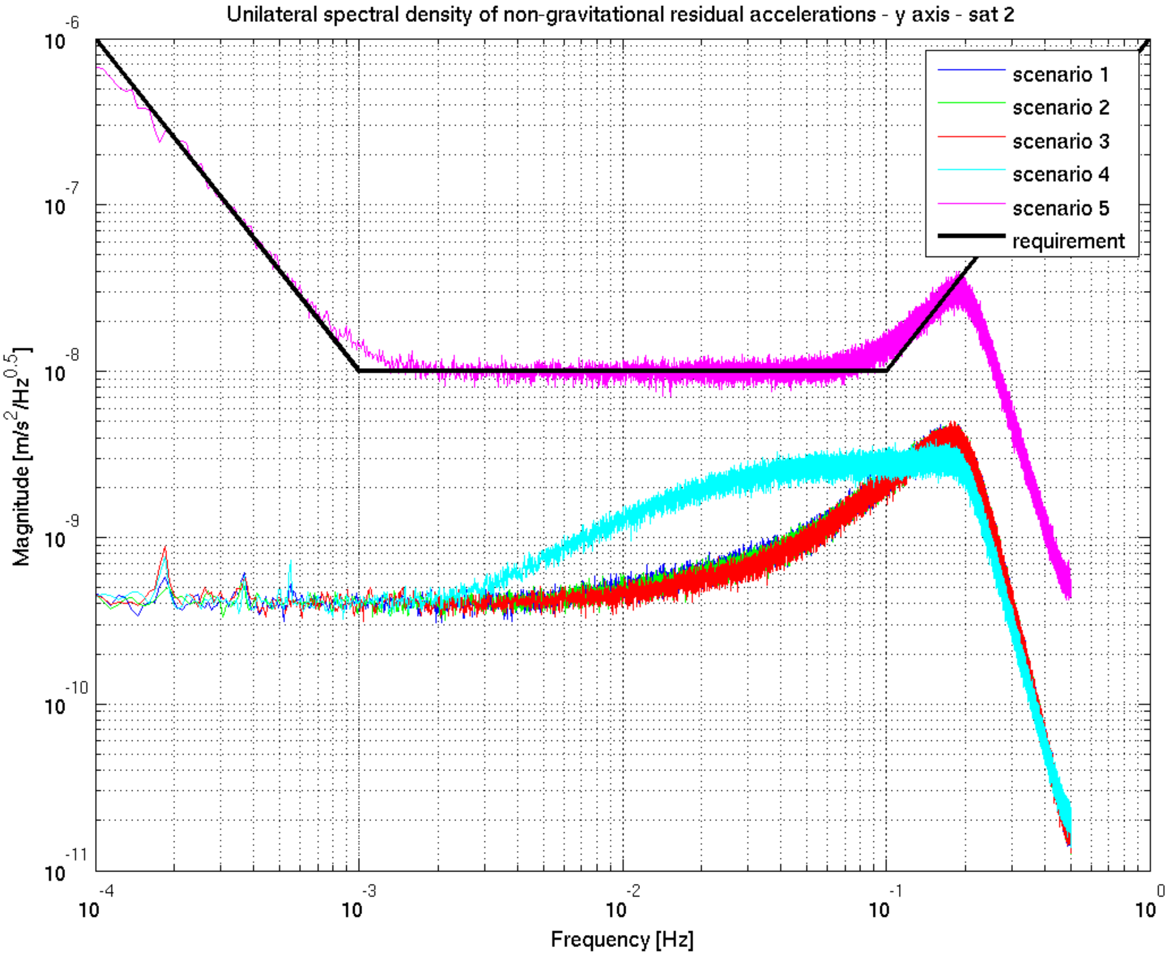


**Figure 4-7: unilateral spectral density of non-gravitational residual accelerations along y axis of satellite 2 for the 5 scenarios.**

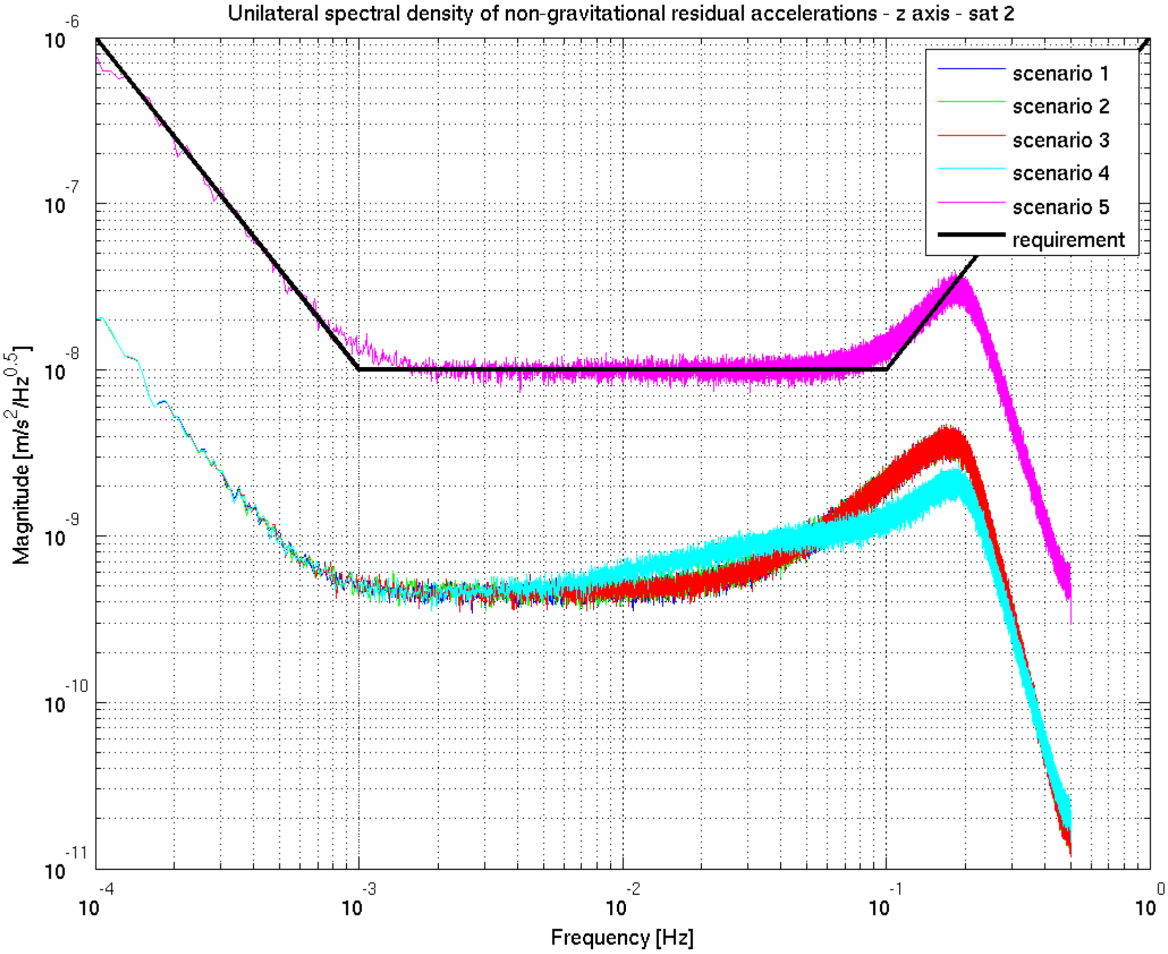


**Figure 4-8: Unilateral spectral density of non-gravitational residual accelerations along z axis of satellite 2 for the 5 scenarios.**

## 4.5 Exchange of information with DEOS

During the preparation of the outputs for the Backward Module, some test simulations have been performed and the results given to DEOS, who checked if the variables present in the output files were sufficiently clear and complete in order for the Backward Module to work correctly. During these interactions, a number of issues came out from both sides, regarding the following subjects:

- attitude angles of the satellites;
- reconstituted variables coming from the "post-facto" emulator;
- parameters used for the computation of the gravity field;
- stability of the cartwheel formation;
- computation of the spectral densities.

All these issues have been successfully resolved. A minor issue regarding an offset in the pitch and yaw angles of the satellites (probably due to a difference in time convention) remains open and will be investigated in the next studies.

# 5. APPENDIX

## 5.1 SS distance measurement error model

The measurement error ( $\delta d$ ) on the satellite-to-satellite distance variation, along the line joining the COM of the two satellites, is generated with the following model:

$$\delta d(t) = \delta d_{J}(t) + \delta d_{\text{others}}(t)$$

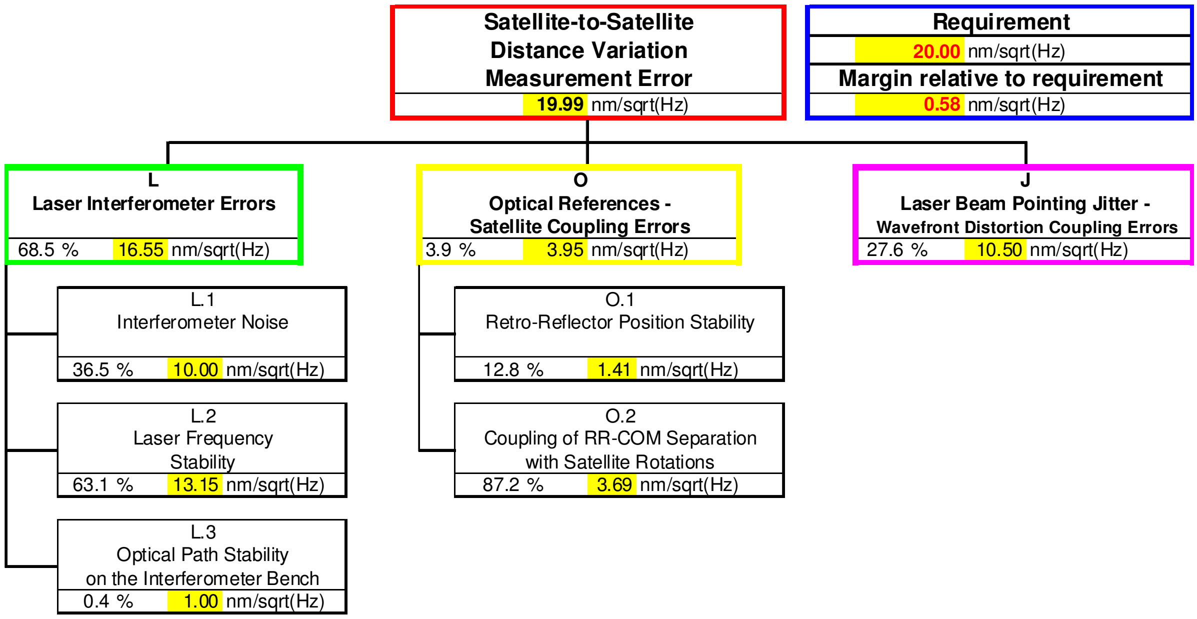


$$\boxed{\delta d_{J}(t) = 185.52 \cdot \left(\theta 1(t) + \psi 1(t)\right) \cdot 2 \times 10^{-5}}$$

$\theta 1(t), \psi 1(t)$ : rotation angles around the Y, Z axes defining the orientation of Satellite 1 in the Satellite-to-Satellite Reference Frame.

$\delta d_{\text{others}}(t)$ must be generated as time series having the following spectral density:

$$\delta d_{\text{others}}(f) = \begin{cases} 1.7 \cdot 10^{-8} & \text{for } f \geq 10^{-2}\ \text{Hz} \\ 1.7 \cdot 10^{-8} \cdot \left(\dfrac{10^{-2}}{f}\right) & \text{for } f < 10^{-2}\ \text{Hz} \\ 1.7 \cdot 10^{-5} & \text{for } f < 10^{-5}\ \text{Hz} \end{cases} \quad \frac{\text{m}}{\sqrt{\text{Hz}}}$$

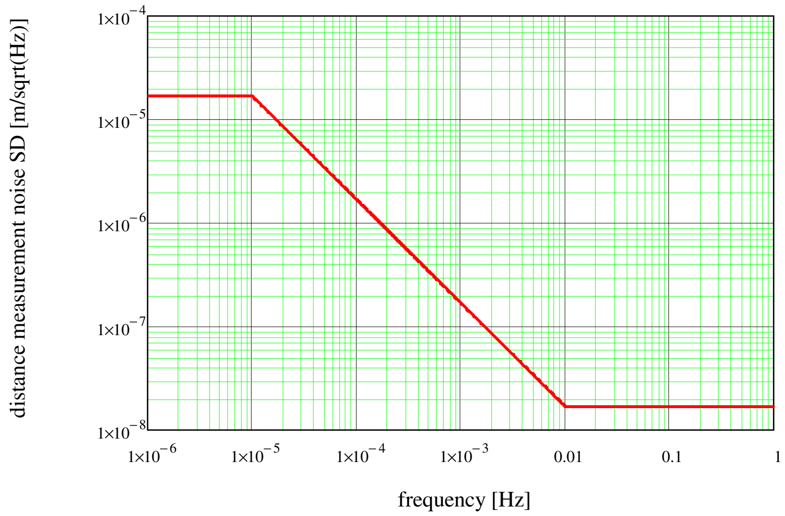


## 5.2 Non-gravitational acceleration measurement error model

The measurement error ($\delta\ddot{d}_D$) on the non-gravitational differential acceleration between the satellites, along the line joining the COM of the two satellites (applicable to a payload consisting of four accelerometer per satellite), is generated with the following model:

$$\delta\ddot{d}_D(t) = \delta\ddot{d}_{C.1}(t) + \delta\ddot{d}_{C.2}(t) + \delta\ddot{d}_{T.2}(t) + \delta\ddot{d}_{\text{others}}(t)$$

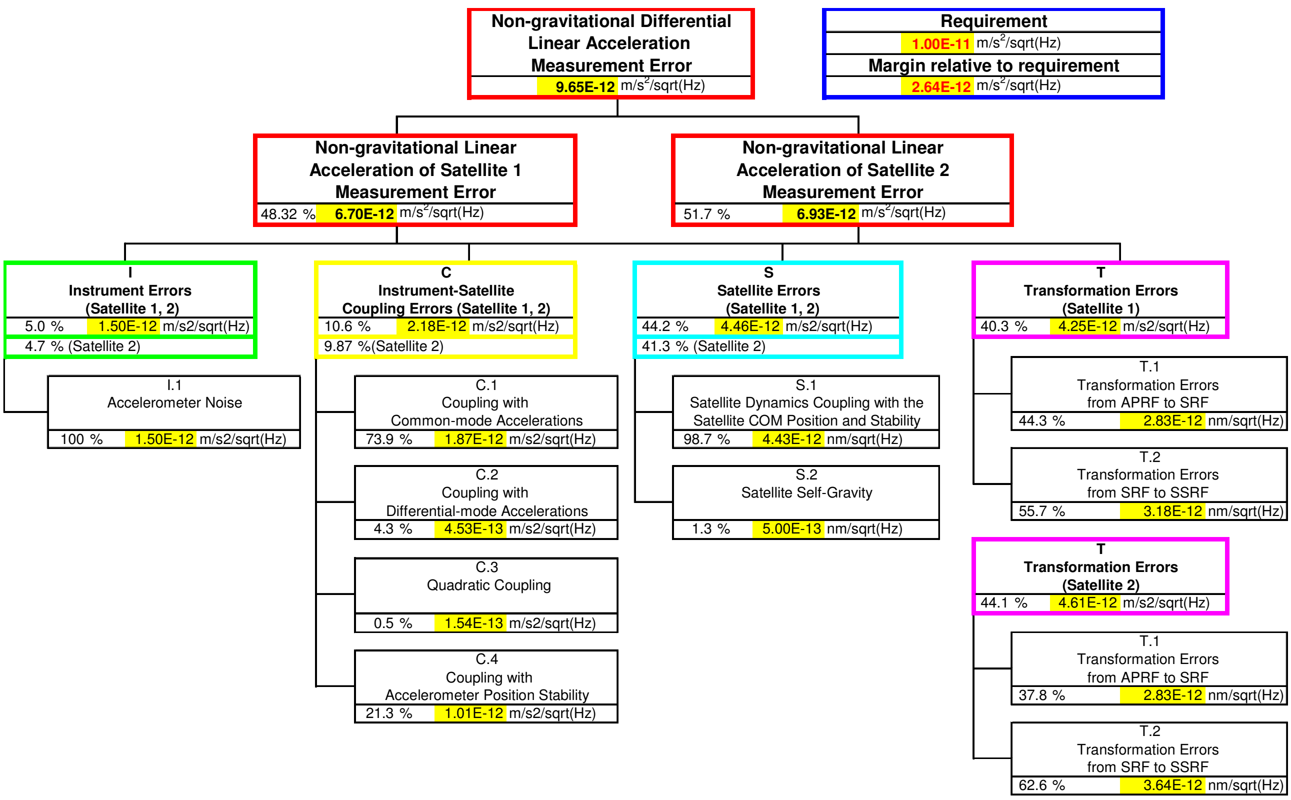

$$\boxed{\delta\ddot{d}_{\mathrm{C.1}}(t)=\sum_{i=1}^{3}\left(\delta MIc_{1,i}\cdot D1(t)_i\right)+\sum_{i=1}^{3}\left(\delta MIc_{1,i}\cdot D2(t)_i\right)}$$

$$\delta MIc=\begin{pmatrix}2\cdot10^{-4} & 1\cdot10^{-4} & 1\cdot10^{-4}\\ 1\cdot10^{-4} & 1\cdot10^{-3} & 1\cdot10^{-4}\\ 1\cdot10^{-4} & 1\cdot10^{-4} & 1\cdot10^{-3}\end{pmatrix}$$

$D1(t)=\begin{pmatrix}D1(t)_{\mathrm{X}}\\ D1(t)_{\mathrm{Y}}\\ D1(t)_{\mathrm{Z}}\end{pmatrix},\ D2(t)=\begin{pmatrix}D2(t)_{\mathrm{X}}\\ D2(t)_{\mathrm{Y}}\\ D2(t)_{\mathrm{Z}}\end{pmatrix}$ : Components of the non-gravitational (drag) accelerations of the COM of Satellite 1 and Satellite 2 in the Satellite Reference Frame

$$\boxed{\delta\ddot{d}_{\mathrm{C.2}}(t)=\frac{1}{2}\left(\delta\ddot{d}11_{\mathrm{C.2}}(t)+\delta\ddot{d}12_{\mathrm{C.2}}(t)\right)+\frac{1}{2}\left(\delta\ddot{d}21_{\mathrm{C.2}}(t)+\delta\ddot{d}22_{\mathrm{C.2}}(t)\right)}$$

$$\delta\ddot{d}11_{\mathrm{C.2}}(t)=\sum_{i=1}^{3}\delta MId_{1,i}\cdot\left(\sum_{j=1}^{3}\left([\Omega1^2(t)]_{ij}+[\dot{\Omega}1(t)]_{ij}\right)\cdot \mathrm{A1}_j\right),\ \delta\ddot{d}12_{\mathrm{C.2}}(t)=\sum_{i=1}^{3}\delta MId_{1,i}\cdot\left(\sum_{j=1}^{3}\left([\Omega1^2(t)]_{ij}+[\dot{\Omega}1(t)]_{ij}\right)\cdot \mathrm{A2}_j\right)$$

$$\delta\ddot{d}21_{\mathrm{C.2}}(t)=\sum_{i=1}^{3}\delta MId_{1,i}\cdot\left(\sum_{j=1}^{3}\left([\Omega2^2(t)]_{ij}+[\dot{\Omega}2(t)]_{ij}\right)\cdot \mathrm{A1}_j\right),\ \delta\ddot{d}22_{\mathrm{C.2}}(t)=\sum_{i=1}^{3}\delta MId_{1,i}\cdot\left(\sum_{j=1}^{3}\left([\Omega2^2(t)]_{ij}+[\dot{\Omega}2(t)]_{ij}\right)\cdot \mathrm{A2}_j\right)$$

$$\delta MId=\begin{pmatrix}2\cdot10^{-4} & 1\cdot10^{-4} & 1\cdot10^{-4}\\ 1\cdot10^{-4} & 1\cdot10^{-3} & 1\cdot10^{-4}\\ 1\cdot10^{-4} & 1\cdot10^{-4} & 1\cdot10^{-3}\end{pmatrix},$$

$\mathrm{A1}=\begin{pmatrix}0\\0.25\\0\end{pmatrix},\mathrm{A2}=\begin{pmatrix}0\\0\\0.25\end{pmatrix}$ : position vectors of accelerometers $A_1$, $A_2$ in the satellite reference frame

$$[\Omega1^2(t)]=\begin{pmatrix}-\omega1_{\mathrm{Z}}^2(t)-\omega1_{\mathrm{Y}}^2(t) & \omega1_{\mathrm{X}}(t)\cdot\omega1_{\mathrm{Y}}(t) & \omega1_{\mathrm{X}}(t)\cdot\omega1_{\mathrm{Z}}(t)\\ \omega1_{\mathrm{X}}(t)\cdot\omega1_{\mathrm{Y}}(t) & -\omega1_{\mathrm{Z}}^2(t)-\omega1_{\mathrm{X}}^2(t) & \omega1_{\mathrm{Y}}(t)\cdot\omega1_{\mathrm{Z}}(t)\\ \omega1_{\mathrm{X}}(t)\cdot\omega1_{\mathrm{Z}}(t) & \omega1_{\mathrm{Y}}(t)\cdot\omega1_{\mathrm{Z}}(t) & -\omega1_{\mathrm{X}}^2(t)-\omega1_{\mathrm{Y}}^2(t)\end{pmatrix},[\dot{\Omega}1(t)]=\begin{pmatrix}0 & -\dot{\omega}1_{\mathrm{Z}}(t) & \dot{\omega}1_{\mathrm{Y}}(t)\\ \dot{\omega}1_{\mathrm{Z}}(t) & 0 & -\dot{\omega}1_{\mathrm{X}}(t)\\ -\dot{\omega}1_{\mathrm{Y}}(t) & \dot{\omega}1_{\mathrm{X}}(t) & 0\end{pmatrix}$$

$\omega1_{\mathrm{X}}(t),\omega1_{\mathrm{Y}}(t),\omega1_{\mathrm{Z}}(t),\dot{\omega}1_{\mathrm{X}}(t),\dot{\omega}1_{\mathrm{Y}}(t),\dot{\omega}1_{\mathrm{Z}}(t)$: angular rates and accelerations of Satellite 1 in SRF
$\omega2_{\mathrm{X}}(t),\omega2_{\mathrm{Y}}(t),\omega2_{\mathrm{Z}}(t),\dot{\omega}2_{\mathrm{X}}(t),\dot{\omega}2_{\mathrm{Y}}(t),\dot{\omega}2_{\mathrm{Z}}(t)$: angular rates and accelerations of Satellite 2 in SRF

$$\boxed{\begin{aligned}\delta\ddot{d}_{\mathrm{T.2}}(t)=&\ \psi1(t)\cdot\delta D1(t)_{\mathrm{Y}}+\delta\psi1(t)\cdot D1(t)_{\mathrm{Y}}+\theta1(t)\cdot\delta D1(t)_{\mathrm{Z}}+\delta\theta1(t)\cdot D1(t)_{\mathrm{Z}}+\\ &\psi2(t)\cdot\delta D2(t)_{\mathrm{Y}}+\delta\psi2(t)\cdot D2(t)_{\mathrm{Y}}+\theta2(t)\cdot\delta D2(t)_{\mathrm{Z}}+\delta\theta2(t)\cdot D2(t)_{\mathrm{Z}}\end{aligned}}$$

$\theta1(t),\psi1(t)$
$\theta2(t),\psi2(t)$ : rotation angles around the Y, Z axes defining the orientation of Satellite 1 and Satellite 2 in the Satellite-to-Satellite Reference Frame.

$D1(t)_{\mathrm{Y}}, D1(t)_{\mathrm{Z}}$ : Components of the non-gravitational (drag) accelerations of the COM

$D2(t)_Y, D2(t)_Z$ of Satellite 1 and Satellite 2 along the Y, Z axes of the Satellite Reference Frame

$\delta\theta 1(t), \delta\psi 1(t)$ : measurement error of $\theta 1(t), \psi 1(t)$
$\delta\theta 2(t), \delta\psi 2(t)$ : measurement error of $\theta 2(t), \psi 2(t)$

$\delta\theta 1(t), \delta\psi 1(t), \delta\theta 2(t), \delta\psi 2(t)$ must be generated as time series having the following spectral density:

$$\begin{matrix}\delta\theta 1(f)\\ \delta\psi 1(f)\end{matrix} = \begin{cases} 1\cdot 10^{-6} & \text{for } f \geq 10^{-3}\ \text{Hz} \\ 1\cdot 10^{-6}\cdot\left(\dfrac{10^{-3}}{f}\right)^2 & \text{for } f < 10^{-3}\ \text{Hz} \\ 0.01 & \text{for } f < 10^{-5}\ \text{Hz} \end{cases} ; \quad \begin{matrix}\delta\theta 2(f)\\ \delta\psi 2(f)\end{matrix} = \begin{cases} 2\cdot 10^{-6} & \text{for } f \geq 10^{-3}\ \text{Hz} \\ 2\cdot 10^{-6}\cdot\left(\dfrac{10^{-3}}{f}\right)^2 & \text{for } f < 10^{-3}\ \text{Hz} \\ 0.02 & \text{for } f < 10^{-5}\ \text{Hz} \end{cases} \quad \frac{\text{rad}}{\sqrt{\text{Hz}}}$$

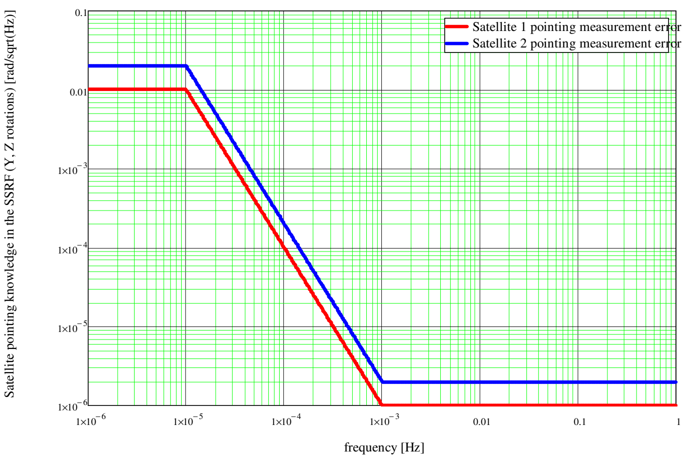


$\delta D1(t)_Y, \delta D1(t)_Z$ : measurement error of $D1(t)_Y, D1(t)_Z$
$\delta D2(t)_Y, \delta D2(t)_Z$ : measurement error of $D2(t)_Y, D2(t)_Z$

$\delta D1(t)_Y, \delta D1(t)_Z, \delta D2(t)_Y, \delta D2(t)_Z$ must be generated as time series having the following spectral density:

$$\begin{matrix}\delta D1(f)_Y\\ \delta D2(f)_Y\end{matrix} = \begin{cases} 1.77\cdot 10^{-11} & \text{for } f \geq 10^{-3} \text{ and } f \leq 0.1\ \text{Hz} \\ 1.77\cdot 10^{-11}\cdot\left(\dfrac{10^{-3}}{f}\right)^2 & \text{for } f < 10^{-3}\ \text{Hz} \\ 1.77\cdot 10^{-11}\cdot\left(\dfrac{f}{0.01}\right)^2 & \text{for } f > 0.1\ \text{Hz} \\ 1.77\cdot 10^{-7} & \text{for } f < 10^{-5}\ \text{Hz} \end{cases} ; \quad \begin{matrix}\delta D1(f)_Z\\ \delta D2(f)_Z\end{matrix} = \begin{cases} 1.84\cdot 10^{-11} & \text{for } f \geq 10^{-3} \text{ and } f \leq 0.1\ \text{Hz} \\ 1.84\cdot 10^{-11}\cdot\left(\dfrac{10^{-3}}{f}\right)^2 & \text{for } f < 10^{-3}\ \text{Hz} \\ 1.84\cdot 10^{-11}\cdot\left(\dfrac{f}{0.01}\right)^2 & \text{for } f > 0.1\ \text{Hz} \\ 1.84\cdot 10^{-7} & \text{for } f < 10^{-5}\ \text{Hz} \end{cases} \quad \frac{\text{m}}{\text{s}^2\sqrt{\text{Hz}}}$$

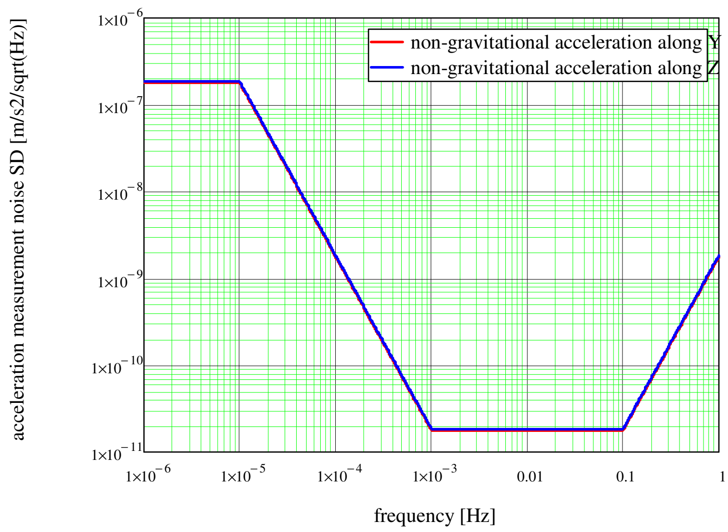


| |
|---|
| $\delta\ddot{d}_{\text{others}}(t)$ must be generated as time series having the following spectral density: |

$$\delta\ddot{d}_{\text{others}}(f) = \begin{cases} 7.89\cdot10^{-12} & \text{for } f \geq 10^{-3} \text{ and } f \leq 0.1\,\text{Hz} \\ 7.89\cdot10^{-12}\cdot\left(\dfrac{10^{-3}}{f}\right)^2 & \text{for } f < 10^{-3}\,\text{Hz} \\ 7.89\cdot10^{-12}\cdot\left(\dfrac{f}{0.01}\right)^2 & \text{for } f > 0.1\,\text{Hz} \\ 7.89\cdot10^{-8} & \text{for } f < 10^{-5}\,\text{Hz} \end{cases} \quad \frac{\text{m}}{\text{s}^2\sqrt{\text{Hz}}}$$

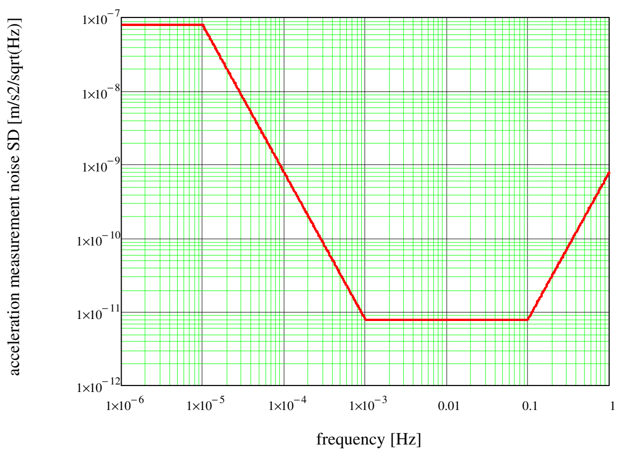

## 5.3 ACRONYMS

| | |
|---|---|
| ACC | Accelerometer |
| ACS | Attitude Control System |
| AD | Applicable Document |
| BOL | Beginning of Life |
| BSM | Beam Steering Mechanism |
| CDMU | Command and Data Management Unit |
| CGE | Cumulative Geoid Error |
| COM | Centre of Mass |
| DFC | Drag Free Control |
| E2E | End-to-End |
| EOL | End of Life |
| EWLT | Equivalent Water Layer Thickness |
| FC | Formation Control |
| GIA | Glacial Isostatic Adjustment |
| GNSS | Global Navigation Satellite System |
| GOCE | Gravity field and steady-state Ocean Circulation Explorer |
| GPS | Global Positioning System |
| GRACE | Gravity Recovery And Climate Experiment |
| INRIM | Istituto Nazionale di Ricerca Metrologica |
| IPA | Ion Propulsion Assembly |
| ITT | Invitation To Tender |
| KBR | K-Band Ranging |
| LEO | Low Earth Orbit |
| ll-SST | low-low Satellite to Satellite Tracking |
| LORF | Local Orbital Reference Frame |
| LRR | Laser Retro Reflector |
| MBW | Measurement Bandwidth |
| MST | Mission Simulation Tool |
| NGGM | Next-Generation Gravity Mission |
| PCDU | Power Control and Distribution Unit |
| P/L | Payload |
| POD | Precise Orbit Determination |
| PSD | Power Spectral Density |
| RD | Reference Document |
| RF | Radio Frequency |
| RIT | Radiofrequency Ion Thruster |
| RMS | Root Mean Square |
| S/C | Spacecraft |
| SLR | Satellite Laser Ranging |
| SOW | Statement of Work |
| SSO | Sun Synchronous Orbit |
| SST | Satellite to Satellite Tracking |
| STR | Star Tracker |
| TAS-I | Thales Alenia Space Italia |
| TBC | To Be Confirmed |
| TBD | To Be Defined |
| TN | Technical Note |
| TT&C | Tracking Telemetry and Command |
| WP | Work Package |

END OF DOCUMENT